

See discussions, stats, and author profiles for this publication at: <https://www.researchgate.net/publication/259869952>

Roles of Inherent Fine Included Mineral Particles in the Emission of PM₁₀ during Pulverized Coal Combustion

ARTICLE *in* ENERGY & FUELS · OCTOBER 2012

Impact Factor: 2.79 · DOI: 10.1021/ef300211u

CITATIONS

9

READS

23

4 AUTHORS, INCLUDING:



[Xiangpeng Gao](#)

Curtin University

30 PUBLICATIONS 318 CITATIONS

SEE PROFILE

Roles of Inherent Fine Included Mineral Particles in the Emission of PM₁₀ during Pulverized Coal Combustion

Xiangpeng Gao,[†] Yi Li,[†] Manuel Garcia-Perez,[‡] and Hongwei Wu^{*,†}

[†]Department of Chemical Engineering and Fuels and Energy Technology Institute, Curtin University, GPO Box U1987, Perth WA 6845, Australia

[‡]Biological Systems Engineering, Washington State University, L. J. Smith 205, P.O. Box 64120, Pullman, Washington 99164-6120, United States

ABSTRACT: A coal sample was prepared from a Western Australia sub-bituminous coal via density separation (1.4–1.6 g/cm³) and size separation (63–90 μm). The mineral matter in the coal is of included nature, of which ~90% are fine mineral particles <10 μm. The raw coal was then washed by dilute acid to prepare an acid-washed coal from which char sample was generated in a quartz drop-tube/fixed-bed reactor at 1000 °C under argon atmosphere. The acid-washed coal and char samples were then combusted in a drop-tube furnace at 1400 °C in air. The PM₁₀ samples collected (mostly PM_{1–10}) contains mainly refractory species including Si, Al, Fe, Mg, and Ca and account for ~19.4% of the total ash collected in both the low-pressure impactor and the cyclone. This suggests important roles of the abundant fine included mineral particles originally present in coal. The significant roles of fine included mineral particles in PM_{1–10} emission during acid-washed coal and char combustion are also clearly evidenced with the presence of abundant individual but partially molten quartz ash particles in the PM_{1–10} range. PM_{0.1} contains dominantly volatile elements (e.g., Na, K, P, S, and Cl) and refractory elements (Fe and Si), while PM_{0.1–1} are mainly composed of Al, Fe, and Si. The significant roles of fine included kaolinite and/or Al-silicates particles in the emission of PM_{0.1–1} from char combustion are also observed. The results suggest that liberation and transformation of fine included mineral particles in coal/char during combustion is a key mechanism responsible for PM₁₀ formation and/or emission. Experimental evidence further suggests that the fine included minerals within a burning coal particle clearly experience coalescence to form large agglomerated ash particles.

1. INTRODUCTION

Inorganic particulate matter (PM) with an aerodynamic diameter less than 10 μm (PM₁₀) is a major aerosol pollutant emitted from stationary coal-fired power stations, drawing worldwide attention due to its adverse health and environmental impacts. The need for controlling PM emission leads to extensive investigations on the formation and/or emission mechanisms of PM₁₀ during coal combustion over the past decade. Several mechanisms are proposed to be responsible for the formation of PM with an aerodynamic size less than 1 μm (PM₁), including inorganic species vaporization, condensation, and aggregation,^{1,2} surface ash shedding during char combustion,^{3,4} bursting of cenosphere,^{5,6} and convective transport of organically bound and possibly small-grained inorganic species away from coal particle during coal devolatilization,⁷ etc. The proposed mechanisms for the formation and/or emission of PM with an aerodynamic size between 1 and 10 μm (PM_{1–10}) from coal combustion are included minerals coalescence,^{8,9} char fragmentation,^{10,11} and excluded minerals fragmentation.^{4,12,13} The particle size distributions (PSDs) and characteristics of PM₁₀ may therefore be governed by a combination of these mechanisms, largely dependent on combustion conditions and coal properties,^{11,14} particularly the characteristics of mineral matter in coal.^{15,16}

In Western Australia (WA), Collie coal is the only coal currently being mined, and it plays an important role in supplying cheap energy to power the state's economy. It is a sub-bituminous coal of high-moisture and high-volatile contents. A unique feature of the coal is that it contains abundant fine

included mineral matter particles (e.g., fine quartz and kaolinite particles, etc.) which are known to be responsible for ash deposit initiation and growth.¹⁷ As results of the presence of these fine mineral matter particles, it is reasonable to speculate that these fine included mineral particles in the coal matrix may substantially contribute to PM₁₀ formation and/or emission during coal combustion. Unfortunately, little work thus far has been done on this important aspect. Therefore, the objective of this study is to use Collie coal as a unique coal sample that is known to contain abundant fine included mineral matter particles for investigating the roles of these mineral particles in the emission of PM₁₀ during coal combustion using a drop tube furnace (DTF).

2. EXPERIMENTAL SECTION

2.1. Samples. To understand the transformation of fine included mineral matter during coal combustion, the key challenge is to obtain a coal sample that contains fine included mineral matter only. In this study, Collie coal was first sampled from the mine site in Collie, WA, crushed, and sieved to prepare a coal sample of density fractions 1.4 – 1.6 g/cm³ via sink-float method, followed by washing with acetone to remove the heavy liquid remained after density separation. The coal sample was then dried in argon at 105 °C for 2 h to completely evaporate the acetone. After that, the coal sample was then sieved to a size fraction of 63–90 μm, termed as “raw coal”. As excluded minerals generally have

Received: February 4, 2012

Revised: June 21, 2012

Published: October 17, 2012



much higher densities ($>2.4 \text{ g/cm}^3$),¹⁸ the raw coal sample contains only included mineral matter, as either discrete included mineral particles or organically bound inorganic elements. To further isolate the contributions of fine discrete included mineral particles and organically bound elements to PM formation during coal combustion, the raw coal sample was then washed using dilute acid (0.1 M HCl) for 24 h and subsequently rinsed with Milli-Q water repeatedly to prepare an acid-washed coal sample for further pyrolysis and combustion experiments. Washing coal with dilute acid removes acid soluble inorganic species (mainly organically bound elements, plus acid soluble minerals such as carbonates, etc.), yielding a coal sample consisting of only discrete included mineral particles.

A char sample was also prepared from the fast pyrolysis of the acid-washed coal at 1000 °C using a quartz drop-tube/fixed-bed reactor,¹⁹ using argon as carrier gas (UHP, 1.5 L min⁻¹). About 1 g of coal particles was fed into the pyrolysis reactor in 20 min at a feeding rate of $\sim 0.05 \text{ g min}^{-1}$. The reactor was then held in the furnace for 10 min before it was lifted out of the furnace and cooled rapidly, with argon continuously flowing through the reactor. The residence time of coal particles in the isothermal zone of the reactor was $\sim 1 \text{ s}$. Hereafter, the char derived from the acid-washed coal is simply referred as “char”. Table 1 lists the main properties of the raw coal, acid-washed coal, and char samples.

Table 1. Properties of Coal and Char Samples

	raw coal	acid-washed coal	char prepared from acid-washed coal (termed as “char”)
Proximate Analysis			
M ^a (% ad)	6.0	6.5	6.8
ash (% db)	5.6	5.1	7.8
VM ^b (% db)	37.8	37.3	3.8
FC ^c (% db)	56.6	57.6	88.4
Ultimate Analysis (% daf)			
C	70.6	71.4	95.0
H	4.00	3.92	0.41
N	1.74	1.96	1.96
S	0.68	0.69	0.12
O ^d	22.98	22.03	2.51
Contents of Inorganic Species (wt % db)			
Si	1.3774	1.2168	1.8605
Al	0.8140	0.7357	1.1762
Fe	0.3368	0.2488	0.4514
Ca	0.0580	0.0480	0.0869
Mg	0.0208	0.0163	0.0280
K	0.0453	0.0171	0.0189
Na	0.0078	0.0063	0.0066
P	0.0680	0.0590	0.0964
Ba	0.0281	0.0184	0.0289
Sr	0.0213	0.0177	0.0279
Ti	0.0498	0.0435	0.0761

^aMoisture. ^bVolatile matter. ^cFixed carbon. ^dBy difference.

2.2. Combustion Experiments and PM Sampling. A DTF system, which was used in recent studies on PM emission from biomass/biochar combustion,^{20–22} was deployed to study the combustion of acid-washed coal and char at a furnace temperature of 1400 °C. The detailed description of the system can be found elsewhere.²⁰ The primary and secondary air flow rates were 1.0 and 4.6 L min⁻¹, respectively. The fuel (coal and char) feeding rate was $\sim 0.05 \text{ g min}^{-1}$. The residence time of fuel particles in the isothermal zone of the DTF was adjusted to be $\sim 1.5 \text{ s}$ in all combustion experiments to achieve complete combustion. The sampling of particulate matter in the combustion flue gas followed a procedure described elsewhere.²⁰ Briefly, the PM₁₀-containing flue gas was firstly separated by a cyclone to collect coarse ash particles (aerodynamic diameter $>10 \mu\text{m}$), then directed to a Dekati low-pressure impactor (DLPI) and its backup filter for size-

segregated collection of PM₁₀. The sampling system (including diluter, cyclone, DLPI, and the sampling lines) was kept at $\sim 115 \text{ °C}$, which was the temperature of the flue gas at the exit of quench sampling probe, in order to avoid possible acid gas condensation and suppress particle coagulation during the sampling process.²⁰

2.3. Sample Analysis and Characterization. The raw coal, acid-washed coal, and char samples were also ashed, digested, and then quantified for determining inorganic species contents using an inductively coupled plasma-atomic emission spectroscopy (ICP-AES), following a procedure detailed elsewhere.¹⁹ The contents of inorganic species in raw coal, acid-washed coal, and char samples were also summarized in Table 1. It is clear that Si, Al, and Fe are the dominant inorganic elements, although other minor elements such as Ca, Mg, K, and P are also present. For the PM samples, the mass-based PSDs were obtained by determining the mass of PM collected in each stage of DLPI using a Mettler MX5 microbalance (accuracy: 0.001 mg). The PM samples were then digested and analyzed using ICP-AES, following the same procedure aforementioned. Selected PM_{1–10} samples and ash samples collected in cyclone were also characterized using a Zeiss EVO 40XVP scanning electron microscopy instrument equipped with an energy dispersive X-ray spectrometer (SEM-EDS) for morphology and chemistry analysis. Selected PM₁ samples from char combustion were also analyzed using a Zeiss Neon EsB focused ion beam scanning electron microscopy (FIBSEM) to achieve a better resolution. A Bruker-AXS D8 advance type X-ray diffractometer (XRD) was used for mineralogy investigation via Cu radiation and a LynxEye position sensitive detector in a 2θ range from 5 to 60°.

3. RESULTS AND DISCUSSION

3.1. Characterization of Fine Mineral Particles in Raw Coal. A series of density-fractioned coal samples were analyzed using computer-controlled scanning electron microscopy (CCSEM), with the detailed data to be reported in another publication.²³ The CCSEM data on fine mineral particles in the coal sample with a density fraction of 1.4–1.6 g/cm³ are plotted in Figure 1. It can be seen in Figure 1a that $\sim 56\%$ and 90% of the total mineral particles are in the form of fine mineral particles with a size $<5 \mu\text{m}$ and a size $<10 \mu\text{m}$, respectively. The coal (density: 1.4–1.6 g/cm³) predominantly contains included mineral matter, as either discrete included mineral particles or organically bound inorganic elements, because excluded minerals generally have much higher densities ($>2.4 \text{ g/cm}^3$)¹⁸ and would not be included in the sample after density separation. Therefore, the abundant fine mineral particles are all fine included mineral particles inherently present within the coal matrix. As shown in Figure 1b, quartz, kaolinite, and iron-bearing minerals are found to be key minerals and the presence of K Al-silicate is also evident. It should be noted in Figure 1 that $\sim 33\%$ of mineral particles are categorized as “unclassified”. A close examination suggests that an “unclassified” mineral particle typically consists of multiple mineral phases, mainly as mixtures of Fe and Ca Al-silicates, plus some Ti- and P-containing minerals to a lesser extent.

Figure 2 further presents the elemental distribution of mineral matter after the raw coal was washed with 0.1 M HCl acid. As expected, the majority of Al and Si are retained in the acid-washed coal, suggesting that Al and Si are not organically bound in the coal matrix but mainly in acid-insoluble forms as included discrete mineral particles. Meanwhile, only small amounts (0.5–1.7%) of K, Mg, S, and Ti are washable by dilute acid, indicating that K, Mg, and Ti are also mainly present in acid-insoluble forms such as aluminosilicates. S may organically occur in the coal substance²⁴ and/or in the mineral fraction such as sulphides, which are acid-insoluble.²⁵ However, Figure 2 shows that 7.1–33.0% of Ca, Sr, Ba, Na, P, and Fe were removed by acid washing,

suggesting that small proportions of these elements are present in the raw coal in either organically bound forms and/or acid-soluble minerals (e.g. carbonates and phosphates). It is known that Na, Ca, Sr, Ba, Fe, and P may be organically bound in coal (particularly low-rank coals) and/or exist as carbonates^{26,27} and phosphates.²⁸

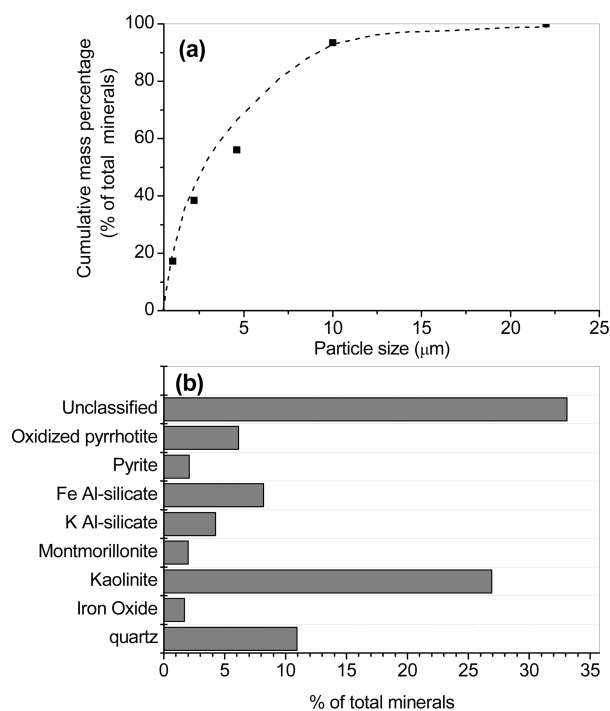


Figure 1. Properties of mineral matter in the coal of density fraction 1.4–1.6 g/cm³: (a) total mineral size distribution; (b) main mineral phases. The data plotted in this figure are derived from the detailed coal CCSEM data to be reported in another publication.²³

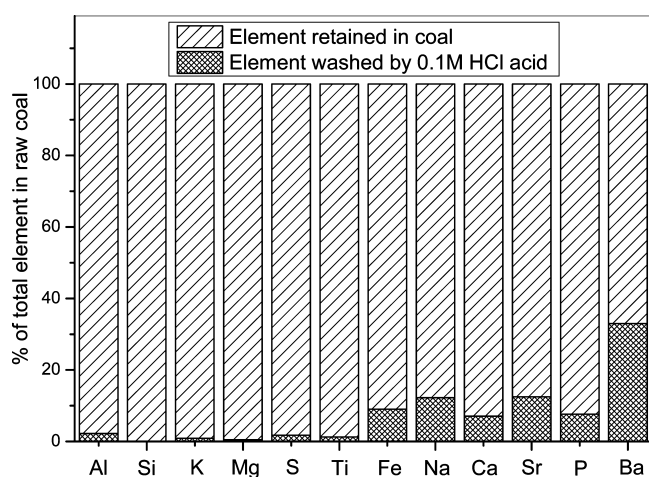


Figure 2. Distribution of inorganic elements in coal after washing with 0.1 M HCl acid.

Based on the data in Figures 1 and 2, it is clear that the raw coal contains abundant fine included mineral particles, plus possibly small proportions of organically bound ash-forming species. Therefore, acid-washing indeed removes the acid-soluble mineral matter and produces a unique coal sample that contains only discrete included mineral particles. Such a unique sample property enables us to purposely investigate the effect of

included mineral matter particularly the fine discrete included mineral particles on PM₁₀ emission.

3.2. Yield and Mass-Based PSDs of PM₁₀ from the Combustion of Coal and Char. Figures 3 and 4 present the yields and PSDs of PM₁₀ produced from the combustion of acid-washed coal and char in the DTF. It should be noted that the ash contents in the acid-washed coal and char are 5.1 and 7.8% db, respectively (see Table 1). Therefore, the PM data were then normalized to the unit mass of ash input in order to directly compare the ability of mineral matter in different fuels on PM₁₀ emission. As shown in Figure 3, the yields of PM₁₀ from the combustion of acid-washed coal and char are 150.1 and 142.6 mg/g ash input, respectively. It is clear that the PM₁₀ contains dominantly PM_{1–10} with yields of 136.2 and 125.9 mg/g ash from the combustion of acid-washed coal and char, respectively. The yields of PM₁ are small (acid-washed coal: 13.9 mg/g ash; char: 16.7 mg/g ash). This is not surprising because the majority of organically bound elements, which are expected to have significant contribution to PM₁ emission,²⁹ would have been already removed by acid washing of the raw coal.

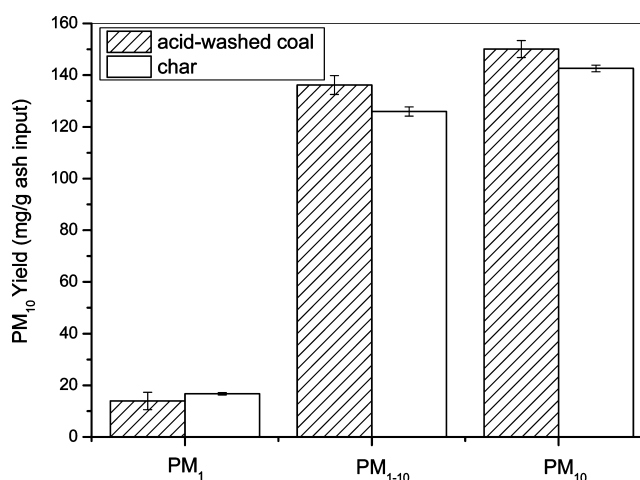


Figure 3. Yield of PM with aerodynamic diameters <1 μm (PM₁), between 1 and 10 μm (PM_{1–10}), and less than 10 μm (PM₁₀) from the combustion of acid-washed coal and char.

The mass-based PSDs of PM₁₀ (see Figure 4) from the combustion of acid-washed coal and char exhibit a bimodal distribution with a coarse mode diameter of ~4.087 μm, which is in agreement with the reported values in previous studies^{30,31} on PM₁₀ from coal combustion, and a fine mode diameter in the range ~0.022–0.043 μm (see the zoom-in figure in Figure 4). Further mass balance analysis indicates that given a collect efficiency of ~68% achieved in sample collection of the DTF system, the amounts of PM₁ and PM_{1–10} account for ~2.3% and ~19.4% based on the total ash collected in DLPI and cyclone (see Figure 5). Particular attentions were then given to PM_{1–10} due to its high proportion in ash, which appears to correlate well with the unique feature of mineral matter in the acid-washed coal samples, that is, the occurrence of abundant fine included mineral particles.

3.3. Direct Evidence on the Significant Contribution of Fine Included Mineral Particles to PM_{1–10} Emission. As discussed in Section 3.2, the high mass proportion of PM_{1–10} based on the total ash collected indicates a good correlation with the occurrence of abundant fine included mineral particles in acid-washed coal and char samples. Furthermore, Figure 6c

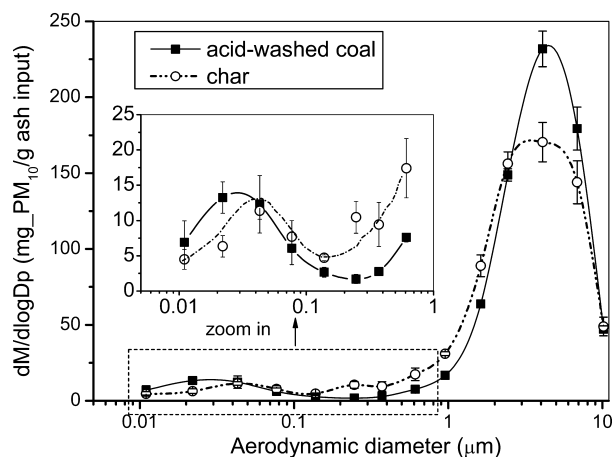


Figure 4. Mass-based particle size distribution (PSD) of PM_{10} from the combustion of acid-washed coal and char.

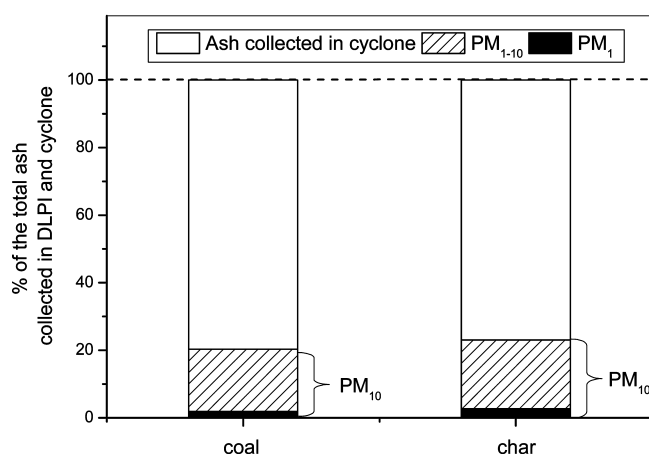


Figure 5. Yield distribution of PM with aerodynamic diameters less than $1 \mu\text{m}$ (PM_1), between 1 and $10 \mu\text{m}$ (PM_{1-10}), and ash collected in cyclone from the combustion of acid-washed coal and char.

shows that the PM_{1-10} samples contain dominantly refractory elements (including Si, Al, Fe, Mg, and Ca) and alkali metals (Na and K). Reported as oxides, the sum of SiO_2 , Al_2O_3 , Fe_2O_3 , MgO , CaO , Na_2O , and K_2O contribute to close to 95.0% of the total mass of PM_{1-10} . Results on water leaching of PM_{1-10} samples show that majorities (89.3–99.0%) of Na and K in PM_{1-10} from the combustion of both acid-washed coal and char are water-insoluble, indicating the forms of Na and K in PM_{1-10} are probably Na- and K- aluminosilicates and/or silicates, rather than salts. Indeed, the chemistry of PM_{1-10} correlated well with that of the mineral matter in the parent fuels (i.e., acid-washed coal and char, see Table 1 and Figure 1b), such data further suggest that the fine included mineral particles are the main source of PM_{1-10} emission.

Efforts were then taken to investigate PM_{1-10} morphology. Figure 7 presents a typical SEM image acquired from the ash particles present in the size fraction of $4.087\text{--}6.852 \mu\text{m}$ in the PM_{1-10} sample from acid-washed coal combustion. The fine ash particles are dominantly spherical- and/or oval- shaped. The energy dispersive X-ray spectra (EDS, see Figure 7) of selected fine ash particles suggest that the spherical particles (also with smooth surfaces) contain mainly Si, Al, Fe, K, and O, possibly as mullite and/or aluminosilicates, indicating these particles have experienced complete melting during combustion. This is not surprising given the abundant kaolinite and Al-silicates particles in coal (see Figure 1b) and the burning coal particles are known to reach a peak temperature several hundred degrees higher than the surrounding gas temperature.^{32,33} The oval-shaped particles contain Si and O only, suggesting these fine ash particles are originated from the abundant fine included quartz (SiO_2) particles in coal but have only experienced partial melting during combustion. Furthermore, XRD diffractograms of the PM_{1-10} samples clearly show that the mineral phases in PM_{1-10} are mainly quartz, mullite, plus aluminum phosphate and iron silicates (see Figure 8). Although the quantitative analysis of mineral phases in PM_{1-10} is difficult to achieve due to limited samples available, the XRD diffractograms clearly suggest the presence of abundant quartz particles in PM_{1-10} .

The results presented in Figures 6–8 have significant implications in revealing the fundamental formation/emission mechanisms of PM_{1-10} during coal combustion. As quartz particles in PM_{1-10} are not likely to be the product of other

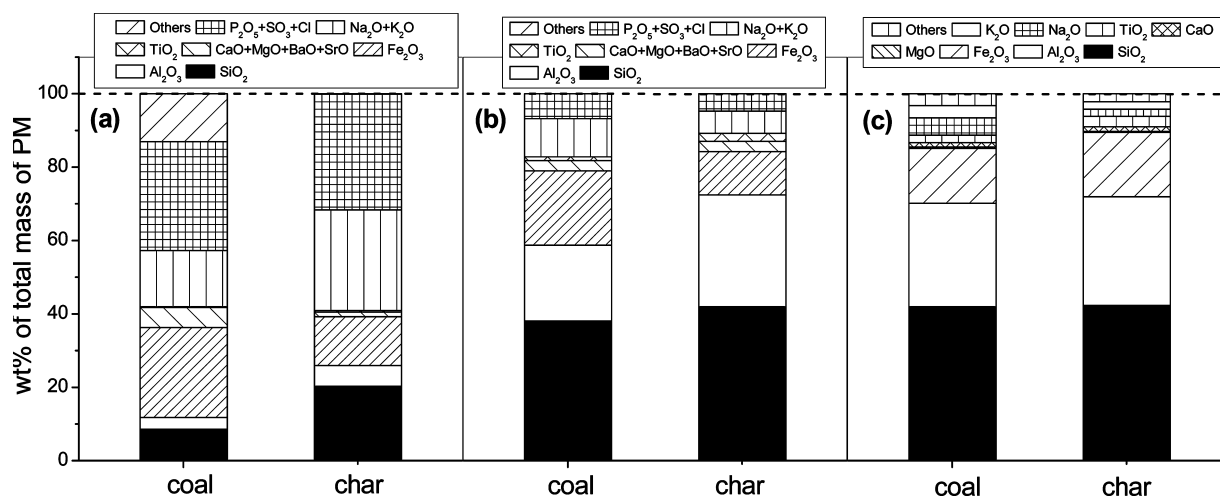


Figure 6. Composition of major inorganic elements (reported as oxides) in (a) $PM_{0.1}$, (b) $PM_{0.1-1}$, and (c) PM_{1-10} collected from the combustion of acid-washed coal and char.

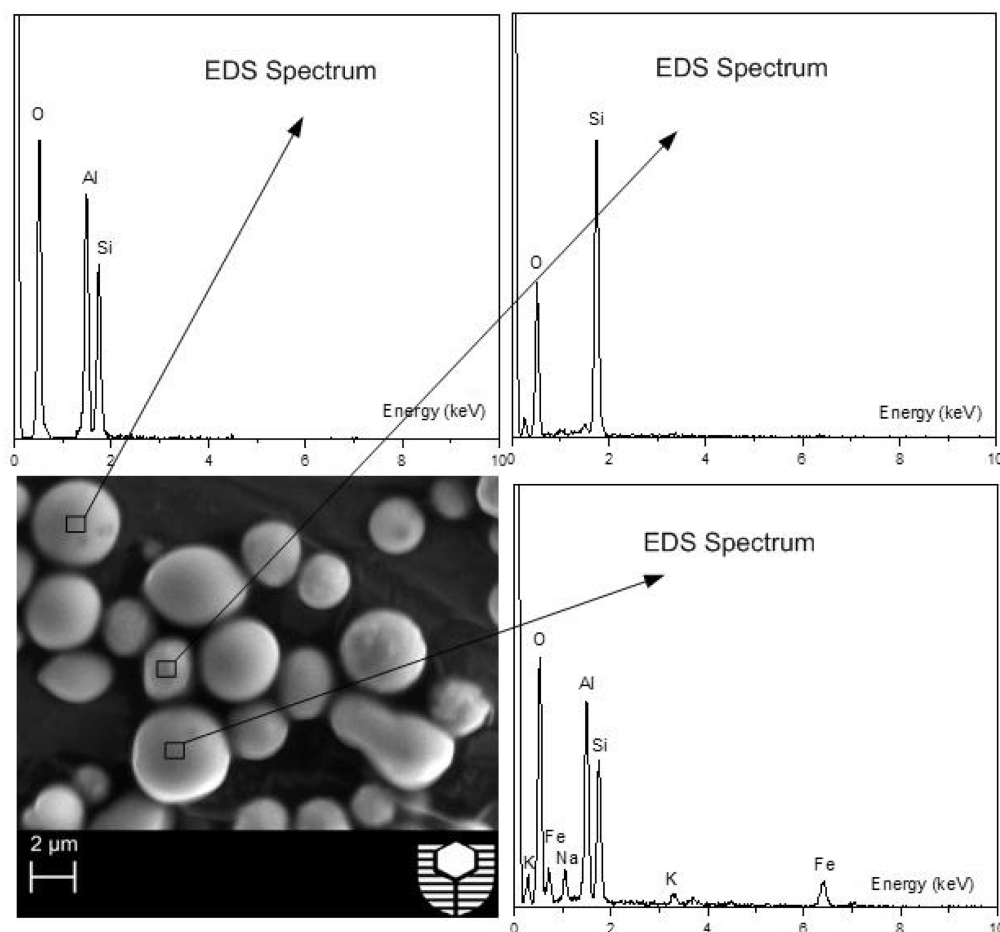


Figure 7. SEM image and EDS spectra of PM with an aerodynamic diameter of 4.087–6.852 μm in PM_{1-10} collected from acid-washed coal combustion.

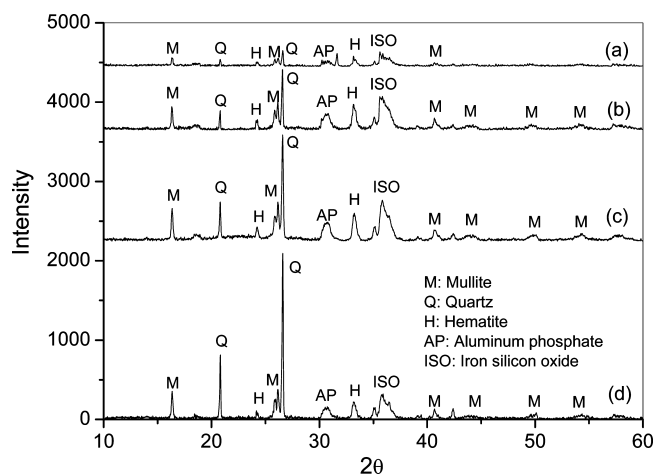


Figure 8. XRD patterns of PM with an aerodynamic diameter of (a) 1.624–2.438 μm , (b) 2.438–4.087 μm , (c) 4.087–6.852 μm , and (d) 6.852–10.174 μm collected from acid-washed coal combustion.

reactions of coal mineral matter during combustion, all the fine quartz ash particles in PM_{1-10} must be formed from the direct transformation of the fine included quartz particles originally present as discrete included mineral matter in the parent fuels (acid-washed coal or char samples). It was reported that fragmentation of quartz (particularly included quartz in coal particles) are unlikely during pulverized coal combustion.¹⁸ The morphology of quartz particles in Figure 7 also suggests that

although they experienced partial melting during combustion, the quartz particles are largely individual ash particles with little evidence of coalescence with other quartz particles included in the same burning coal particles. Therefore, the results in Figures 6–8 provide direct experimental evidence for direct transformation of fine discrete included quartz mineral particles into fine quartz ash particles in PM_{1-10} as an important mechanism for PM_{1-10} formation.

Similarly, it is therefore also possible that the contribution of other fine mineral particles (such as fine kaolinite, Fe Al-silicates, pyrite etc.) in coal to PM_{1-10} formation/emission can also be substantial, although different mineral reactions and various extents of coalescence of these fine included mineral particles may take place within the burning coal particles. This is clearly supported by the major mineral phases identified in PM_{1-10} , as shown in Figure 8. For example, mullite is known to be the major product of kaolinite thermal decomposition.¹⁸ The presence of hematite in PM_{1-10} is a clear indication on the direct transformation of pyrite combustion with minimal coalescence with other ash particles.

3.4. Roles of Inherent Fine Included Mineral Particles in PM_1 Emission. Recent studies^{29,34,35} suggest that PM_1 can be divided into two major fractions including PM with an aerodynamic diameter of less than 0.1 μm ($\text{PM}_{0.1}$) and 0.1–1 μm ($\text{PM}_{0.1-1}$), both organically bound metals and the inherent fine mineral particles in coal are proposed to play important roles in their formation and/or emission. Therefore, the chemical compositions of $\text{PM}_{0.1}$ and $\text{PM}_{0.1-1}$ collected from the

combustion of acid-washed coal and char are presented in panels (a) and (b) of Figure 6, respectively. As expected, $PM_{0.1}$ from both acid-washed coal and char combustion dominantly contains volatile elements (e.g., Na, K, P, S, and Cl), followed by refractory elements such as Fe and Si, while the amounts of Al and other alkaline earth metals (e.g., Ca, Mg, Ba, and Sr) are limited. For instance, the sum of Cl and oxides of Na, K, P, and S contributes to $\sim 45.0\%$ and $\sim 59.0\%$ of the total mass of $PM_{0.1}$ collected from the combustion of acid-washed coal and char, respectively. The oxides of Fe and Si account for $\sim 33.3\%$ to the total mass of $PM_{0.1}$ for both acid-washed coal and char combustion. Oppositely, $PM_{0.1-1}$ is mainly composed of refractory elements (Al, Si, and Fe), the oxides of which account for $\sim 78.9\%$ and $\sim 84.3\%$ to the total $PM_{0.1-1}$ collected from the combustion of acid-washed coal and char, respectively, while the amounts of volatile elements such as Na, K, P, S, and Cl are relatively low. Indeed, such an obvious discrepancy on the composition of $PM_{0.1}$ and $PM_{0.1-1}$ indicates that their formation and/or emission are governed by different mechanisms.

The PSDs of refractory elements such as Al and Si are normally adopted to reveal the formation and/or emission mechanisms of PM_1 produced from coal combustion.^{29,35} In addition, the organically bound metals in raw coal were removed by dilute acid washing as aforementioned (see Section 3.1). To further isolate the contribution of volatiles (including the inorganic species carried out by volatiles) combustion to PM_1 emission,²¹ the PSDs of Al and Si in PM_1 produced from char combustion are presented in Figure 9 to purposely investigate the contribution of vaporization-condensation of included minerals and direct transformation of inherent fine mineral particles to PM_1 emission during char combustion. There are two key findings from the data shown in Figure 9. On one hand, increasing particle size leads to a gradual increase in the mass of Si and Al in $PM_{0.1}$, but a drastic increase of those in $PM_{0.1-1}$, which are in agreement with the higher contents of both Al and Si in $PM_{0.1-1}$ compared with those in $PM_{0.1}$ (see panels a and b of Figure 6). On the other hand, the mass of Al in $PM_{0.1}$ is much lower than that of Si; however, the PSDs of Al and Si start to follow a similar trend in $PM_{0.1-1}$.

The data in panels (a) and (b) of Figure 6 and Figure 9 provide important insight into the mechanisms responsible for the formation and/or emission of $PM_{0.1}$ and $PM_{0.1-1}$ during acid-washed coal and/or char combustion. The volatile elements such as Na, K, P, S, and Cl in PM_1 , particularly in $PM_{0.1}$, are generally known^{3,11,36} to be formed via vaporization of these elements at high temperature during solid fuels combustion, followed by series of gas phase reactions, homogeneous nucleation, and/or heterogeneous condensation, and/or reaction in surface of existing particles. Particle coagulation and agglomeration may also be involved.³⁷ A close examination shows that only 28.3% of total P in $PM_{0.1}$ is in form of phosphate (PO_4^{3-}) during coal combustion, indicating majority of P in $PM_{0.1}$ is in water-insoluble form (e.g. the mixture of P with aluminosilicates).³⁸ This further confirms the heterogeneous reactions between the P-containing vapor and other existing particles such as Al- and/or Si-containing particles. On the contrast, for refractory species (e.g., Fe, Al, and Si) in $PM_{0.1}$, a generally accepted mechanism for the vaporization of these oxides is the reduction to more volatile metal (Fe) and suboxides (AlO and SiO) under the locally reducing atmosphere in fuel-rich regions and within the burning-char particles.² Furthermore, a recent study on pyrite combustion³⁹ suggests that extensive fragmentation of ash cenospheres may also contribute to the formation and/or

emission of $PM_{0.1}$. CCSEM data illustrate the presence of pyrite in raw coal sample (see Figure 1b); therefore, it is reasonable to speculate that part of Fe in $PM_{0.1}$ may be contributed by fragmentation of cenospheres (if any) during coal and/or char combustion. In addition, Al is suggested to be harder to vaporize compared with Si,²⁹ explaining well with the dominant existence of SiO_2 , rather than Al_2O_3 in $PM_{0.1}$ (see Figures 6a and 9). Lastly, the Si in $PM_{0.1}$ seems to be contributed from fine included Si-containing mineral particles (such as quartz particles) in the coal/char via two possible mechanisms. One is that these fine quartz particles provide substantial surface area for reduction reaction within the burning coal/char particle, enhancing the release of SiO that would be further reoxidized in the flame zone to form SiO_2 fume. The other is that there are possibly ultrafine inherent quartz particles (e.g., those $<0.1\ \mu m$) in the coal. The direct liberation of such ultrafine quartz (if any) can lead to the formation of $PM_{0.1}$. Direct liberation of ultrafine inherent mineral particles appears to be possible. The morphology of PM samples in $0.043\text{--}0.077\ \mu m$ size fraction from char combustion is shown in Figure 10a, apart from the spherical or aggregate-like particles as results of vaporization-condensation mechanism, the existence of oval-shaped and individual particle is also evident, suggesting the direct liberation of ultrafine mineral particles.

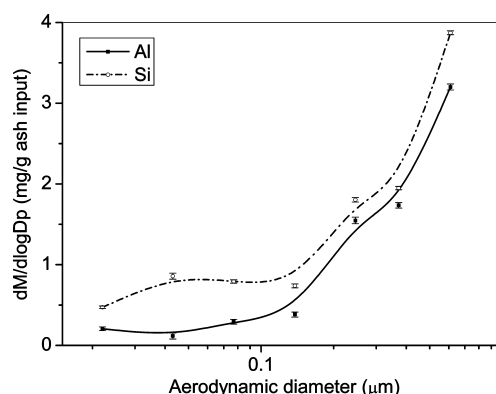


Figure 9. Elemental mass-based particles size distribution of Al and Si in PM_1 collected from char combustion.

Opposite of $PM_{0.1}$, both Si and Al are dominantly contained in $PM_{0.1-1}$; furthermore, the PSD of Al corresponds closely to that of Si in the size range $0.1\text{--}1\ \mu m$ (see Figures 6b and 9). Such data clearly suggest the direct transformation of fine (about $1\ \mu m$) Al- and Si-containing mineral particles (such as Al-silicates, montmorillonite and kaolinite, see Figure 1b) into $PM_{0.1-1}$. Furthermore, the molar ratio of Si/Al in $PM_{0.1-1}$ is ~ 1.16 , which is much lower compared to the ratio of ~ 3.11 in $PM_{0.1}$. Such a substantial decrease in Si/Al molar ratio in $PM_{0.1-1}$ compared to that in $PM_{0.1}$ further confirms the different transformation mechanisms of Al-containing minerals into $PM_{0.1}$ and $PM_{0.1-1}$. For example, Al in $PM_{0.1}$ is likely to be a result of limited vaporization and condensation,² while the direct transformation of fine Al- and Si-containing minerals seems to be responsible for the abundance of both Al and Si in $PM_{0.1-1}$. Additionally, such a molar ratio (~ 1.16) of Si/Al in $PM_{0.1-1}$ suggests the dominant existence of aluminosilicates in $PM_{0.1-1}$, as the molar ratio of Si/Al in majority of aluminosilicates such as Na- and K-aluminosilicates is known to be ~ 1 . The existence of aluminosilicates in $PM_{0.1-1}$ is also indicated by the EDS analysis of selected spherical particle with size range $0.61\text{--}0.955\ \mu m$, as shown in Figure 10b. Considering the data presented in Figure

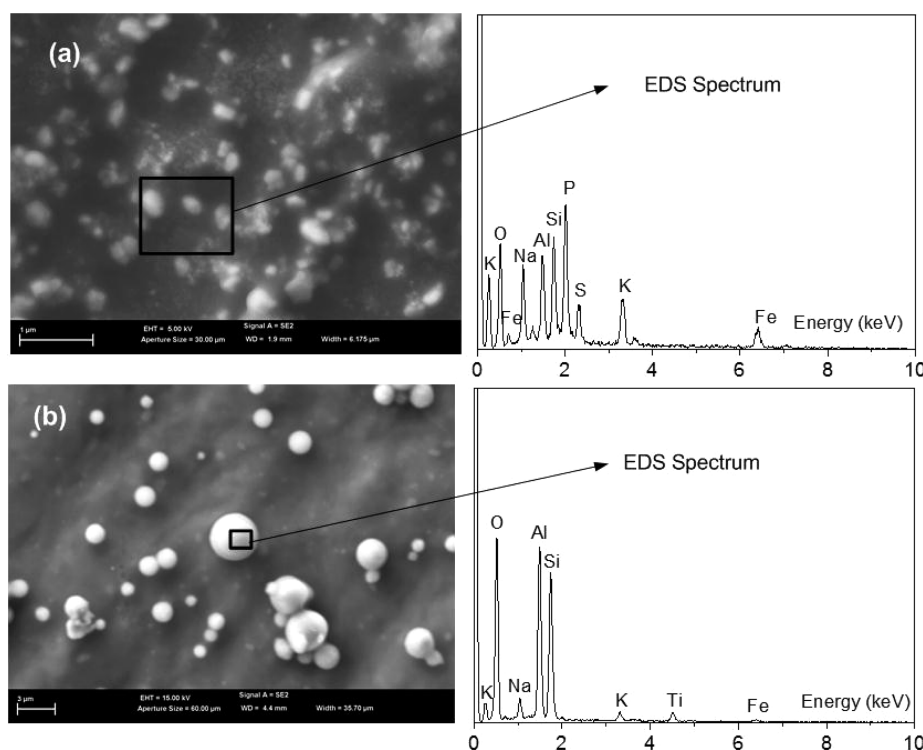


Figure 10. SEM images and EDS spectra of PM with an aerodynamic diameter of (a) 0.043–0.077 μm and (b) 0.61–0.955 μm in PM_{10} collected from char combustion.

6b and Figures 9–10 together, it is clear that Al in $\text{PM}_{0.1-1}$ is originated from the fine (about 1 μm) Al- and Si-containing mineral particles presented in char, and it is most likely to exist as aluminosilicates in $\text{PM}_{0.1-1}$ as a result of a series of mineral reactions during char combustion.

It should be noted that the fine mineral particles in char may come from two parts. One is the fine mineral particles originally existed in coal. Indeed, CCSEM data have shown that about 17% of the total mineral particles are in the form of particles with a size around 1 μm (see Figure 1a). The other may be the fine mineral particles produced during char preparation. In fact, the char was prepared at 1000 $^{\circ}\text{C}$, the primary decompositions of included mineral matters such as kaolinite¹⁸ and/or pyrite⁴ (see Figure 1b) are likely to take place to fragment into smaller mineral particles, probably accompanied by char fragmentation. Overall, the transformation of inherent fine particles (particularly kaolinite and/or Al-silicates) originally existed in the coal, and/or the fine mineral particles produced during char preparation plays a significant role in $\text{PM}_{0.1-1}$ emission.

In summary, the results in Sections 3.3 and 3.4 clearly indicate that the inherent fine included mineral particles originally presented in parent fuels (acid-washed coal and char) can substantially contribute to the formation and/or emission of fine ash particles in PM_{10} (including both PM_1 and PM_{1-10}). This finding is of practical importance because it shows that the properties (e.g., PSDs and mineral compositions) of inherent fine mineral matter in coal may also need to be considered as a key criterion in coal selection guideline for assessing the potential of a particular coal in forming PM_{10} during combustion.

3.5. Possible Mechanisms Responsible for the Discrepancies in the Emission Behavior of PM_{10} from the Combustion of Acid-Washed Coal and Char. It is also noteworthy that there are apparent discrepancies in the emission behavior and characteristics of PM_{10} from the combustion of

acid-washed coal and char (see Figures 3 and 4). The PSD of PM_{10} (particular at sizes between 0.1 and 2.438 μm) from char combustion appears to slightly shift to smaller sizes in comparison to that from acid-washed coal combustion, accompanied by a considerable reduction in the mass yield of PM with a size range 4.087–10.174 μm . Consequently, the yields of PM_{1-10} from char combustion are $\sim 5.3\%$ lower than that from the combustion of its parent coal. However, the difference in the yields of PM_1 from the combustion of acid-washed coal and char seems to be within the experimental error.

There may be at least two possible mechanisms that may be responsible for the differences in the emission of PM_{1-10} between char and acid-washed coal combustion. One is the absence of volatile matter in a char compared to its parent coal. During coal pyrolysis, the release of volatiles may be accompanied by the volatilization of inorganic species. Considering the char yield (51.8% db) and the contents of major inorganic species (Si, Al, Fe, Na, K, Mg, Ca, P, and S) in char or acid-washed coal samples (see Table 1), the retentions of these species are determined and presented in Figure 11. It can be seen that the majorities (80–98%) of Si, Al, Fe, Mg, Ca, and P were retained in char with only 2–20% of these species were released during pyrolysis. About 44.3% of Na and K and 90% of S were also released during acid-washed coal pyrolysis. The releases of these species during pyrolysis may be partially responsible for the slight reduction in the yields of PM_{1-10} during char combustion.

The other is the possible differences in the combustion conditions between char combustion and its parent coal combustion. The intensified release of volatiles during coal combustion would lead to rapid rotations of burning coal particles.⁴⁰ Therefore, such rotations would be much faster for burning coal particles during coal combustion in comparison to the burning char particles, leading to enhanced shedding of ash particles from the receding surface of fuel particle hence

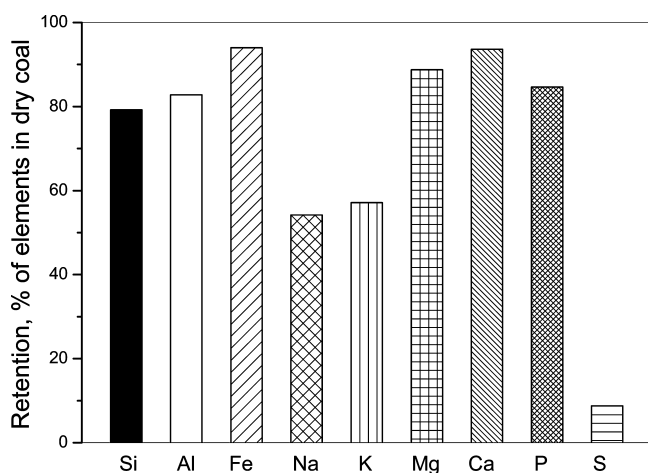


Figure 11. Retention of major inorganic elements in char produced from fast pyrolysis of acid-washed coal at 1000 °C.

increased PM_{1-10} yield. Additionally, the absence of volatiles combustion during the combustion of char also leads to a lower particle temperature during char combustion.^{41–43} A lower combustion temperature is known to result in the weakened shedding of ash particles from burning coal/char particles and the decreased liberation of fine included mineral particles within a burning coal/char particle.¹⁵ As a result, the fine included mineral particles would have increased time to coalesce, leading to decreased PM_{1-10} yield during char combustion. Indeed, as shown in Figure 12, coalescence of included mineral particles in burning char/coal particles obviously took place during coal/char combustion because there are substantial amounts of large ash agglomerates ($>10\ \mu\text{m}$) present in the ash samples collected in the cyclone from the combustion of either acid-washed coal or

char. The intensified coalescence and agglomeration of fine included mineral particles during char combustion are also clearly evidenced because the ash agglomerates collected in cyclone from char combustion are considerably bigger than those from coal combustion.

4. CONCLUSIONS

This paper reports the significant roles of fine included mineral particles in the formation and/or emission of PM_{10} during the combustion of pulverized coal and char. The main conclusions are drawn as follows:

- (1) CCSEM results show that $\sim 56.0\%$ and $\sim 90\%$ of the total mineral particles in the Collie coal sample with a density fraction of $1.4\text{--}1.6\ \text{g/cm}^3$ are fine included mineral particles with sizes less than 5 and $10\ \mu\text{m}$, respectively. The major included minerals are quartz, kaolinite, and iron-bearing minerals.
- (2) The PM_{10} collected from the combustion of acid-washed coal and char samples dominantly contains PM_{1-10} , of which the yields are 136.2 and $125.9\ \text{mg/g}$ ash input for acid-washed coal and char combustion, respectively. However, the yields of PM_1 are limited, of which are 13.9 and $16.7\ \text{mg/g}$ ash input for acid-washed coal and char combustion, respectively. As a result, the amounts of PM_1 and PM_{1-10} account for $\sim 2.3\%$ and $\sim 19.4\%$ of the total ash collected in DLPI and cyclone, respectively, from the combustion of both acid-washed coal and char.
- (3) PM_{1-10} contains dominantly refractory species, including Si, Al, Fe, Mg, and Ca. Na and K, which are mainly in water-insoluble forms, are also evident. The significant roles of fine included mineral particles in PM_{1-10} emission during acid-washed coal and char combustion are clearly

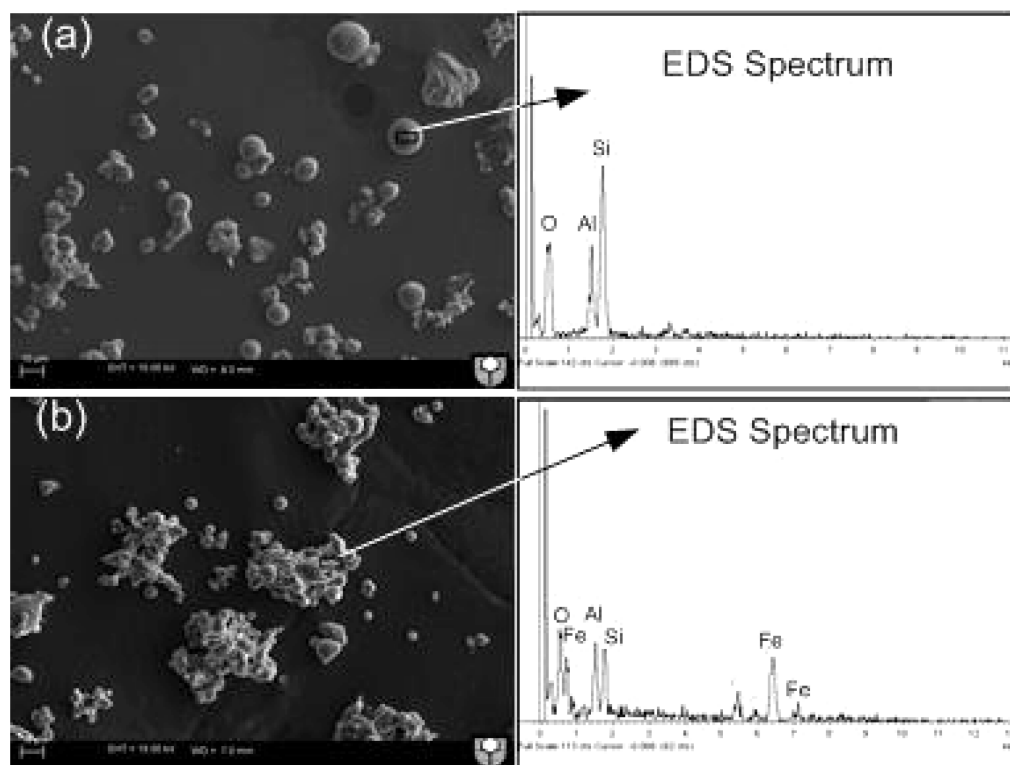


Figure 12. SEM images and EDS spectrum of ash particles collected by cyclone from the combustion of (a) acid-washed coal and (b) char.

evidenced via the identification of the presence of abundant individual but partially molten quartz ash particles in PM_{1-10} .

- (4) PM_1 from the combustion of acid-washed coal and char is composed of two major fractions ($PM_{0.1}$ and $PM_{0.1-1}$) with different chemical compositions. $PM_{0.1}$ dominantly contains volatile elements (such as Na, K, P, S, and Cl) and refractory elements (Fe and Si), with little amounts of Al and other alkaline earth metals (such as Ca, Mg, Ba, and Sr). Oppositely, $PM_{0.1-1}$ is mainly composed of refractory elements (Al, Fe, and Si), which account for ~84.3% of the total $PM_{0.1-1}$ based on the mass of their oxides, while the amounts of volatile elements such as Na, K, P, S, and Cl are relatively low. Furthermore, the significant roles of fine included kaolinite and/or Al-silicates particles in the emission of $PM_{0.1-1}$ from char combustion are also evident based on the vast existence of aluminosilicates in $PM_{0.1-1}$.
- (5) The differences in PSDs and yields of PM_{10} between the combustion of acid-washed coal and char may be due to the release of inorganic species (mainly Si, Al, Fe, Na, K, Mg, Ca, P, and S) during coal pyrolysis for char preparation and the possible differences in their prevailing combustion conditions.

AUTHOR INFORMATION

Corresponding Author

*Telephone: +61-8-92667592. Fax: +61-8-92662681. E-mail: h.wu@curtin.edu.au.

Notes

The authors declare no competing financial interest.

ACKNOWLEDGMENTS

The authors are grateful to the partial support received from the Australian Research Council's Discovery Projects Program. The authors also acknowledge the team led by Prof. Yoshihiko Ninomiya at Chubu University for assistance in coal CCSEM analysis, with the detailed data to be reported in a related publication. Centre for Materials Research at Curtin University's Faculty of Science and Engineering is also acknowledged for access to electron microscope facilities. X.G. is also grateful to the EIPRS and the CUPS scholarships for his PhD study.

REFERENCES

- (1) Neville, M.; Quann, R. J.; Haynes, B. S.; Sarofim, A. F. *Symp. (Int.) Combust.* **1981**, *18*, 1267–1274.
- (2) Quann, R. J.; Sarofim, A. F. *Symp. (Int.) Combust.* **1982**, *19*, 1429–1440.
- (3) Quann, R. J.; Neville, M.; Janghorbani, M.; Mims, C. A.; Sarofim, A. F. *Environ. Sci. Technol.* **1982**, *16*, 776–781.
- (4) Srinivasachar, S.; Helble, J. J.; Boni, A. A. *Prog. Energy Combust. Sci.* **1990**, *16*, 281–292.
- (5) Smith, R. D.; Campbell, J. A.; Nielson, K. K. *Atmos. Environ.* (1967) **1979**, *13*, 607–617.
- (6) Richard D, S. *Prog. Energy Combust. Sci.* **1980**, *6*, 53–119.
- (7) Baxter, L. L.; Mitchell, R. E.; Fletcher, T. H. *Combust. Flame* **1997**, *108*, 494–502.
- (8) Baxter, L. L.; Mitchell, R. E. *Combust. Flame* **1992**, *88*, 1–14.
- (9) Yan, L.; Gupta, R. P.; Wall, T. F. *Fuel* **2001**, *80*, 1333–1340.
- (10) Helble, J. J.; Sarofim, A. F. *Combust. Flame* **1989**, *76*, 183–196.
- (11) Sarofim, A. F.; Howard, J. B.; Padia, A. S. *Combust. Sci. Technol.* **1977**, *16*, 187–204.
- (12) Srinivasachar, S.; Helble, J. J.; Boni, A. A.; Shah, N.; Huffman, G. P.; Huggins, F. E. *Prog. Energy Combust. Sci.* **1990**, *16*, 293–302.
- (13) Yan, L.; Gupta, R.; Wall, T. *Energy Fuels* **2001**, *15*, 389–394.

- (14) Yan, L.; Gupta, R. P.; Wall, T. F. *Fuel* **2002**, *81*, 337–344.
- (15) Buhre, B. J. P.; Hinkley, J. T.; Gupta, R. P.; Nelson, P. F.; Wall, T. F. *Fuel* **2006**, *85*, 185–193.
- (16) Zhang, L.; Ninomiya, Y. *Fuel* **2006**, *85*, 194–203.
- (17) Wee, H. L.; Wu, H.; Zhang, D.-K. *Energy Fuels* **2006**, *21*, 441–450.
- (18) Bryers, R. W. *Prog. Energy Combust. Sci.* **1996**, *22*, 29–120.
- (19) Yip, K.; Tian, F.; Hayashi, J.-i.; Wu, H. *Energy Fuels* **2009**, *24*, 173–181.
- (20) Gao, X.; Wu, H. *Energy Fuels* **2010**, *24*, 4571–4580.
- (21) Gao, X.; Wu, H. *Energy Fuels* **2011**, *25*, 4172–4181.
- (22) Gao, X.; Wu, H. *Energy Fuels* **2011**, *25*, 2702–2710.
- (23) Wu, H.; Gao, X.; Ninomiya, Y.; et al. Occurrence and Characteristics of Abundant Fine Included Mineral Particles in Collie Coal of Western Australia, to be submitted.
- (24) Huffman, G. P.; Mitra, S.; Huggins, F. E.; Shah, N.; Vaidya, S.; Lu, F. *Energy Fuels* **1991**, *5*, 574–581.
- (25) Raask, E. *Prog. Energy Combust. Sci.* **1985**, *11*, 97–118.
- (26) van Dyk, J. C.; Baxter, L. L.; van Heerden, J. H. P.; Coetzer, R. L. *J. Fuel* **2005**, *84*, 1768–1777.
- (27) Miller, S. F.; Schobert, H. H. *Energy Fuels* **1993**, *7*, 1030–1038.
- (28) Greer, R. T. *Coal Microstructure and Pyrite Distribution*, ACS Symposium Series; American Chemical Society: Washington, DC, 1977; Vol. 1.
- (29) Zhang, L.; Ninomiya, Y.; Yamashita, T. *Fuel* **2006**, *85*, 1446–1457.
- (30) Liu, X.; Xu, M.; Yao, H.; Yu, D.; Gao, X.; Cao, Q.; Cai, Y. *Energy Fuels* **2006**, *21*, 157–162.
- (31) Liu, X.; Xu, M.; Yao, H.; Yu, D.; Lv, D.; Zhou, K. *Energy Fuels* **2008**, *22*, 3844–3851.
- (32) Wall, T. F.; Lowe, A.; Wibberley, L. J.; McC. Stewart, I. *Prog. Energy Combust. Sci.* **1979**, *5*, 1–29.
- (33) Saastamoinen, J. J.; Aho, M. J.; Hämäläinen, J. P.; Hernberg, R.; Joutsenoja, T. *Energy Fuels* **1996**, *10*, 121–133.
- (34) Zhang, L.; Ninomiya, Y.; Yamashita, T. *Energy Fuels* **2006**, *20*, 1482–1489.
- (35) Zhuo, J. K.; Li, S. Q.; Yao, Q.; Song, Q. *Proc. Combust. Inst.* **2009**, *32*, 2059–2066.
- (36) Helble, J. J.; Sarofim, A. F. *J. Colloid Interface Sci.* **1989**, *128*, 348–362.
- (37) Xu, M.; Yu, D.; Yao, H.; Liu, X.; Qiao, Y. *Proc. Combust. Inst.* **2011**, *33*, 1681–1697.
- (38) Zhang, L.; Ninomiya, Y. *Proc. Combust. Inst.* **2007**, *31*, 2847–2854.
- (39) Li, Y.; Gao, X.; Wu, H. Roles of Ash Cenosphere Fragmentation in the Formation of Ash and Particulate Matter during Pulverized Pyrite Combustion. PPT presentation at *The 7th International Symposium on Coal Combustion*, Harbin, China, 2011.
- (40) Kang, S.-W.; Sarofim, A. F.; Beér, J. M. *Symp. (Int.) Combust.* **1989**, *22*, 145–153.
- (41) Levendis, Y. A.; Joshi, K.; Khatami, R.; Sarofim, A. F. *Combust. Flame* **2011**, *158*, 452–465.
- (42) Atal, A.; Levendis, Y. A. *Fuel* **1995**, *74*, 1570–1581.
- (43) Bejarano, P. A. *Combust. Sci. Technol.* **2007**, *179*, 1569–1578.